

RESEARCH ARTICLE

Power-Over-Fiber System With Intermittent Operation Based on Capacitor Voltage Estimation for High-Efficiency Energy Charging

TOMOHIRO KAWANO¹, RYO KOYAMA, AKIHIRO KURODA, TAKUI UEMATSU²,
CHISATO FUKAI, HIROSHI WATANABE, AND IKUTARO OGUSHI

NTT Access Network Service Systems Laboratories, NTT Corporation, Tsukuba, Ibaraki 305-0805, Japan

Corresponding author: Tomohiro Kawano (tomohiro.kawano@ntt.com)

ABSTRACT We propose a power-over-fiber system with a new photovoltaic converter voltage control technology consisting of intermittent operation of a light source based on capacitor voltage estimation to achieve high energy efficiency. This efficiency is made possible by ensuring the photovoltaic converter voltage stays within an appropriate range. However, detecting and controlling the voltage on the photovoltaic converter side would waste power. In our system, a controller on the light source side estimates the voltage of photovoltaic converter side from our circuit model and controls the photovoltaic converter voltage by controlling light source activation/deactivation. Therefore, it is possible to maintain high photoelectric conversion efficiency without wasting power on the photovoltaic converter side. We show that this method can significantly improve energy efficiency from 11.0% to 22.4% compared to a method that controls the voltage on the photovoltaic converter side. We also demonstrate that an optical switch with a power consumption of 130 mW can be driven with 5-mW optical input. Our power-over-fiber system is practical because its optical power is low and safe enough to be used in existing optical access networks.

INDEX TERMS Power-over-fiber, single-mode fiber, intermittent operation, photoelectric conversion efficiency, photovoltaic converter.

I. INTRODUCTION

Power-over-fiber (PoF) is a technology that supplies electric power to electrical devices using a photovoltaic converter (PVC) which converts optical power from a light source passed through an optical fiber. Because it has high immunity to electromagnetic noise and low transmission loss of the light, it is a useful power supply system for electrical devices located in outdoors or at locations far from the power source. Many studies have been conducted on PoF systems to obtain high electric power to operate electrical devices by using optical fibers specifically designed for high-power optical transmission or by developing a PVC with high

photoelectric conversion efficiency [1], [2], [3], [4], [5], [6], [7], [8], [9], [10], [11], [12]. As an example of the maximum power supply possible, Matsuura et al. reported that high-power laser-diodes and photovoltaic power converters based on the vertical epitaxial monolithic heterostructure architecture could be combined to supply 43.7 W electric power from a 150 W optical power input via a 300-m double-clad fiber [12]. Other studies on PoF systems used low-power laser diodes (LDs). As an example of the minimum power supply, López-Lapeña et al. used a low-power 2 mW LD to continuously supply 105 μ W electric power to a sensor through a multimode fiber (MMF) [13]. The sensor worked at a sampling frequency of 200 Hz and transmitted 16-bit data via the MMF. Additionally, Roeger et al. used a 2.2 mW optical power input to drive a microelectromechanical

The associate editor coordinating the review of this manuscript and approving it for publication was Shuo Sun.

system (MEMS) optical switch through a single-mode fiber (SMF) [14]. The safety limit of optical power for optical fiber communication systems installed in public areas is specified to be 115 mW by the International Electrotechnical Commission (IEC) [15]. Therefore, these PoF systems are applicable to existing optical access networks. All studies mentioned above operate devices that consume less power than the power supplied by the PoF system.

PoF systems that operate electrical devices whose electric power consumption exceeds the power supplied by the PoF system have been reported. These systems set a capacitor beside the PVC and operate the electrical devices intermittently. For example, Diouf et al. proposed a PoF system that uses to optical power input of 2.5 W to obtain 190 mW of electric power after transiting 8 km of SMF [16]. They operated a sensor with an electric power consumption of 240 mW by charging a capacitor mounted beside the sensor. Mei et al. proposed a system that operated various sensors by the electric energy stored in a capacitor charged by the 226 mW electrical output of a PVC with 10.9 km transmission over SMF [17]. In addition, the authors proposed a PoF system with a capacitor to drive an optical switch with an electric power consumption of 130 mW using a 10-mW light source via SMF [18]. Our PoF system uses safe optical power and so is also applicable to existing optical access networks. However, the energy efficiency of our proposed PoF system was low. The photoelectric conversion efficiency of a PVC depends on the voltage applied to the PVC. However, the voltage of the capacitor depends on the amount of electricity stored. Therefore, in a PoF system using a capacitor, it is necessary to hold the PVC voltage to within an appropriate range in order to maintain high photoelectric conversion efficiency. Diouf et al. set a switching regulator between the PVC and capacitor so that the PVC voltage is not affected by the capacitor voltage [16]. Mei et al. used maximum power point tracking (MPPT) technology to control PVC voltage [17]. However, switching regulators consume energy during voltage conversion, as does MPPT operation. In order to improve the energy efficiency of a PoF system, it is necessary to maintain high photoelectric conversion efficiency and reduce the energy consumed to control PVC voltage.

In this paper, we propose a PoF system with a new PVC voltage control approach that uses intermittent operation of the light source based on estimates of the capacitor voltage on the PVC side to achieve high energy efficiency. In our system, the electric power output by the PVC is directly input to a capacitor mounted beside the PVC, and a controller installed beside the light source controls the light source to keep PVC voltage appropriate to ensure high photoelectric conversion efficiency. Because our system does not need to control the PVC voltage on the PVC side, the energy consumption on the PVC side is reduced while photoelectric conversion efficiency is kept high. In Section II, we describe the circuit model for voltage estimation and experimentally determine the model parameters. In Section III, we confirm the validity of the intermittent operation of the PoF

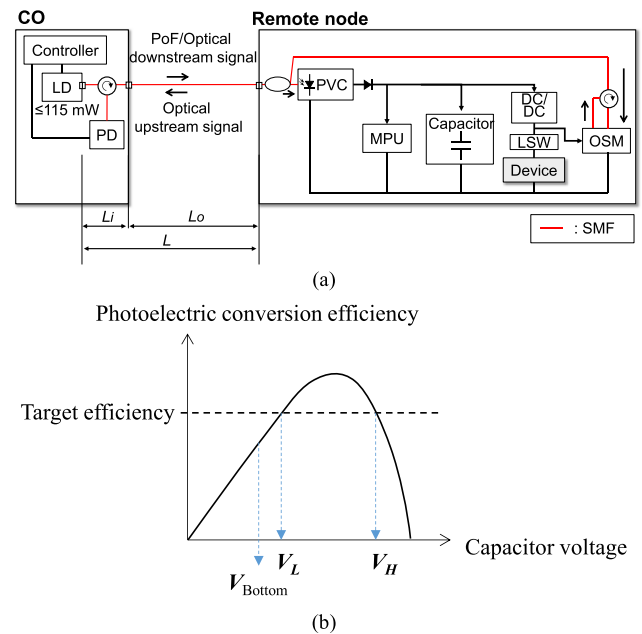


FIGURE 1. (a) Proposed PoF system. (b) Photoelectric conversion efficiency of a PVC directly connected to a capacitor.

system through experiments on a prototype remote node. In Section IV, we demonstrate our PoF system driving an optical fiber switch. Finally, our conclusions are presented in Section V.

II. PROPOSED INTERMITTENT OPERATION CONTROL

A. PRINCIPLE

The basic configuration of the proposed PoF system is shown in Fig. 1(a). A controller, an LD, and a photo diode (PD) are set in a central office (CO). A remote node and an electric device are in the field. The controller controls the remote node via the LD and PD, and the remote node controls the electric device. Regular SMF connects the remote node to the CO. The downward light and upward light are multiplexed and demultiplexed using an optical circulator. A PVC and a capacitor are installed in the remote node to convert the received feeding light into electricity and store it in the capacitor. To prevent the electricity in the capacitor flowing back into the PVC when the driving light is off, a backflow prevention diode is set on the PVC's output. The remote node is also equipped with a micro processing unit (MPU), which processes instructions from the CO. In addition, the electric device and optical signal modulator (OSM) are driven using the stored energy held in the capacitor. To minimize the power consumption of the standby remote node, the MPU goes into sleep mode and the electrical device is inactive. Only when the LD is on and the controller of the CO sends a command to the remote node, is the MPU in sleep mode triggered to wake by the fall of the superimposed signal. The electrical device is then turned on by a load switch (LSW) and the power held by the capacitor is supplied to the device via a

direct current-to- direct current (DC/DC) converter. After the device operation is completed, the completion report is made to the CO, and the MPU enters sleep mode again. The remote node splits the continuous downlink light and modulates part of it in the OSM. The modulated light is returned to CO as the uplink signal light.

The minimum optical received power of the remote node in this configuration is determined as follows. An example, the CO's transmission loss, L_i , is reported to be 3.3 dB in [18]. The SMF line loss of the optical fiber network, including the connection loss, is reported to be 1 dB/km [19]; the outdoor optical fiber line loss L_o was set at 7.0 dB as 99% of public switched telephone network subscriber lines are less than 7 km [20]. Therefore, when the output power of the LD is 115 mW, the minimum light power received at the remote node is 10.7 mW.

Since the PVC and the capacitor are connected, the output voltage of the PVC basically equals the capacitor voltage. The photoelectric conversion efficiency of the typical PVC varies with the output voltage. Fig. 1(b) shows the power conversion characteristics of a PVC directly connected to a capacitor. The vertical and horizontal axes plot the photoelectric conversion efficiency and the voltage of the capacitor, respectively. When light of sufficient intensity is supplied to the PVC, the conversion efficiency of the PVC is linear to the capacitor voltage if the capacitor voltage is under upper threshold V_H . However, when the capacitor voltage exceeds V_H , the efficiency decreases and most of the optical power is wasted. Our previous PoF system continuously supplied optical power from the LD, so when the capacitor voltage exceeded V_H the output power of the PVC saturates. Therefore, the energy stored in the capacitor is very small relative to the energy supplied by the LD, and the efficiency of energy charging was poor. In this paper, the photoelectric conversion efficiency is kept high by intermittent operation of the LD to keep the voltage of the capacitor between V_L and V_H . For this control, it is necessary to know whether the voltage of the capacitor. Usually, in order to know the value, it is necessary for the MPU to measure the capacitor voltage and transmit the measurement result to the CO using OSM. Of course, during this data collection and transfer process, both MPU and OSM consume the energy stored in the capacitor. Therefore, in this paper, instead of using MPU and OSM to monitor the capacitor voltage in the remote node, the capacitor voltage is estimated at the CO side.

B. INTERMITTENT OPERATION

The LD is intermittently operated to keep the photoelectric conversion efficiency high as follows:

- 1) When the electric device is inactive, the on-off operation of the LD keeps the capacitor voltage within the operating voltage range of V_H and V_L .
- 2) During operation of the electric device, the capacitor voltage is maintained between V_H and V_L , even after activation is terminated, to ensure proper start-up voltage and sufficient capacitor charge.

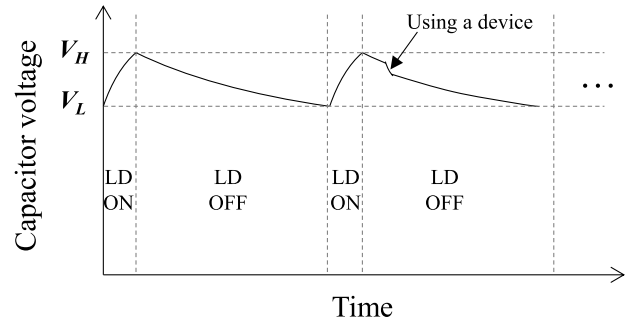


FIGURE 2. Capacitor voltage control using intermittent operation for the remote node.

As shown in Fig. 2, the LD power supply is turned on until the capacitor voltage of the remote node reaches V_H , where upon it is turned off. When the capacitor voltage of the remote node reaches V_L , the LD is turned on again. V_L must be set greater than the minimum driving voltage V_{Bottom} of the MPU. To evaluate the efficiency of the PoF system, we employ the metric of Energy Charging Efficiency, ECE, which is expressed as:

$$ECE = \frac{\text{Energy charged in Capacitor}}{\text{Energy provided by LD}} \quad (1)$$

In this paper, after setting the target value of photoelectric conversion efficiency, ECE is compared between PoF systems with and without intermittent operation. Since the capacitor voltage cannot be estimated in a PoF system without intermittent operation, the LD is controlled by obtaining the capacitor voltage through communication at fixed intervals. In the PoF system with intermittent operation, the capacitor voltage is estimated at the CO side, and LD is activated as appropriate.

C. CIRCUIT MODEL FOR CAPACITOR VOLTAGE ESTIMATION

In order to estimate the capacitor voltage of the remote node, we assumed a circuit model for the electrical circuit part including PVC. Fig. 3 shows the circuit model (a) when charging the capacitor with the LD active and the circuit model (b) when discharging power from the capacitor with the LD turned off. First, the voltage estimation model at the time of charging is explained. In general, from the I-V characteristics of PDs such as PVC, the output current is expressed as [21]:

$$I_{PVC} = -J_0 \left\{ \exp \left(\frac{eV_{PVC}}{nkT} \right) - 1 \right\} + \frac{\eta P_0 e \lambda}{hc} \quad (2)$$

where J_0 , e , V_{PVC} , n , k , T , η , P_0 , λ , h , and c are the inverse saturation current, elementary charge, output voltage of PVC, diode ideal coefficient, Boltzmann's constant, temperature of PVC, quantum efficiency of PVC, the optical input power, the optical input wavelength, Planck's constant, and speed of light, respectively. I_1 and I_2 are the current flowing through the MPU and the current flowing through the

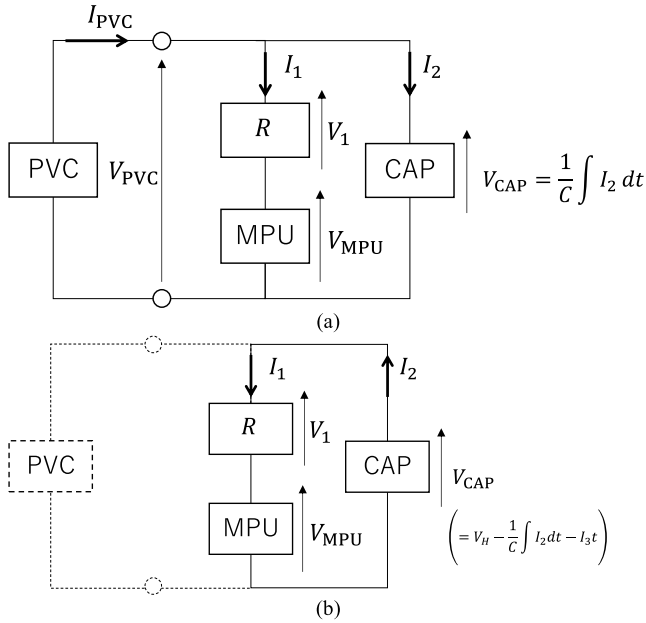


FIGURE 3. (a) Circuit model during charging; (b) Circuit model during discharging. PVC: Photovoltaic converter, MPU: Micro processing unit, CAP: Capacitor.

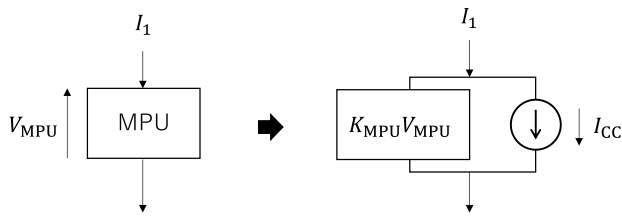


FIGURE 4. Current model for the MPU. MPU: Micro processing unit.

capacitor, respectively. We assumed the I-V characteristic of the MPU are equivalent to those of the circuit shown in Fig. 4. Here, we assumed that although the MPU basically operates in sleep mode, there are two types of currents flowing through the MPU: constant-current I_{CC} and current $K_{MPU}V_{MPU}$, which is proportional to voltage V_{MPU} applied to the MPU. Thus, I_1 is given as follows:

$$I_1 = I_{CC} + K_{MPU}V_{MPU} \quad (3)$$

The I-V relation of capacitors is well known to be

$$V_{CAP} = \frac{1}{C} \int I_2 dt, \quad (4)$$

where I_2 , V_{CAP} , and C are the current flowing through the capacitor, capacitor voltage, and the capacitance, respectively.

Because $V_{PVC} = V_1 + V_{MPU} = V_{CAP}$ and $I_{PVC} = I_1 + I_2$, the following equation is obtained from (1) to (3).

$$\frac{dV_{CAP}}{dt} = -\frac{J_0}{C} \left\{ \exp\left(\frac{eV_{CAP}}{nkT}\right) - 1 \right\} + \frac{\eta P_0 e \lambda}{Chc} - \frac{I_{CC}}{C} - \frac{K_{MPU}(V_{CAP} - RI_{CC})}{C(RK_{MPU} + 1)} \quad (5)$$

where R is the dc resistance of the circuit. Using (5), the capacitor voltage during charging can be estimated by numerical analysis.

Second, we present here the estimation of the capacitor voltage when LD is off, see Fig. 3(b). The discharge of the capacitor starts when voltage V_{CAP} is equal to V_H . V_{CAP} during discharge is well known to be described as follows.

$$V_{CAP} = V_H - \frac{1}{C} \left(\int I_2 dt \right) - \frac{I_3}{C} t \quad (6)$$

Here, I_3 is the leakage current of the capacitor. It occurs in both states of charge and discharge, but the state of charge is ignored in (4) as the charge time is short, so the value is small. Given that $I_2 = I_1$ and $V_1 + V_{MPU} = V_{CAP}$, the following equation can be derived from (3) and (6).

$$\frac{dV_{CAP}}{dt} = -\frac{K_{MPU}}{C(RK_{MPU} + 1)} V_{CAP} + \frac{K_{MPU}RI_{CC}}{C(RK_{MPU} + 1)} - \frac{I_{CC}}{C} - \frac{I_3}{C} \quad (7)$$

Using (7), the capacitor voltage during discharge can be obtained by numerical analysis.

The intrinsic parameters of η , n , J_0 for PVC, and I_{CC} , K_{MPU} for MPU, are derived experimentally. As the PVC and MPU, we adopted KPC8-T, an indium gallium arsenide (InGaAs)-based material, and PIC18LF47K40-I/PT, respectively, as described in Section III. We selected KPC8-T because it can output a voltage sufficient to drive the MPU, 1.8 V or more, at the assumed minimum optical input of 10.7 mW. It has high photoelectric conversion efficiency at optical inputs in the communication wavelength band. Since it is necessary to reduce the standby power consumption of the MPU, to be able to drive the MPU from a low voltage, and to be able to cope with the voltage fluctuation of the capacitor to be charged and discharged, we selected PIC18LF47K40-I/PT for its low power mode; it can be driven at voltages in the range of 1.8-3.6 V. Fig. 5 shows the measurement results of the short-circuit current and the open-circuit voltage of the PVC. The wavelength of the LD used was 1490 nm. Since the slope of the short-circuit current curve in Fig. 5 is $0.1185 \cdot 10^{-3}$ A/W, η is determined to be 0.09875 from (2). From the open-circuit voltage and (2) in Fig. 5, n and J_0 are found to be 8.78 and $3.02 \cdot 10^{-10}$ A, respectively. Fig. 6 shows the measured values of the supply voltage of the MPU and the current consumed by the MPU at the time of discharge (taken from Fig. 3(b)). From Fig. 6, I_{CC} and K_{MPU} were derived as $3.533 \mu\text{A}$ and $9.942 \cdot 10^{-6}$ A/V, respectively. K_{MPU} meets the derived value when it is 2.7 V or more.

III. EXPERIMENT

A. REMOTE NODE PROTOTYPE

We fabricated a remote node prototype and validated the effects of intermittent operation. Fig. 7 shows the fabricated prototype remote node. We employed KPC8-T and PIC18LF47K40-I/PT as PVC and MPU, respectively.

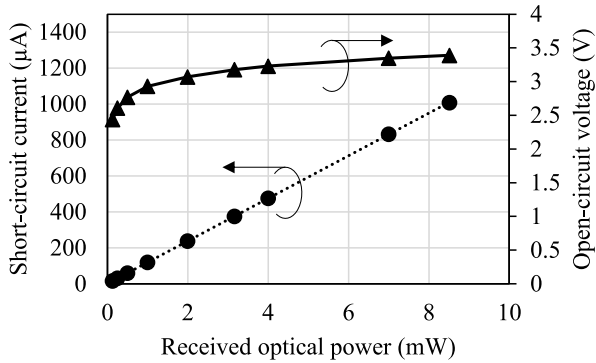


FIGURE 5. Short-circuit current and open-circuit voltage versus optical power received by the PVC.

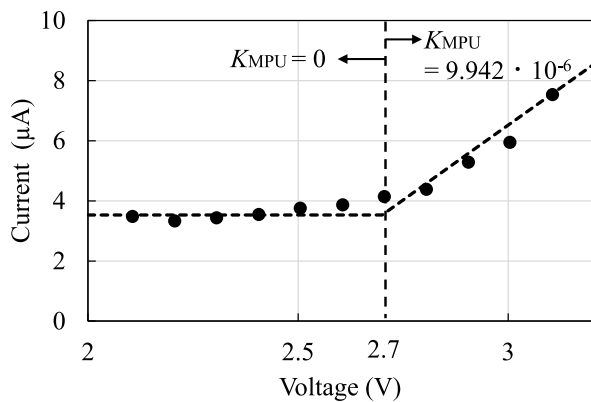


FIGURE 6. Relationship between supply voltage of the MPU and the current consumed by the MPU during discharge.

The LD light source wavelength was 1490 nm. For the capacitor, we used an electric double layer capacitor (EDLC), which is small, has large capacitance, and excellent repetitive charging characteristics. A MEMS optical on/off switch (MS-10-C-O-15-40-9/LT) was employed as the OSM [22]. Its switching time is up to 5 ms, while the PoF system has a universal asynchronous receiver transmitter (UART) interface and can communicate at a data rate of 110 bps. The data transmitted to the CO is the voltage value of the capacitor and the completion notification of the electric device operation. The data rate of 110 bps is sufficient to transmit this data. Moreover, an example of the electric devices being considered, we employed a 1×16 optical switch (LBSW-1165111334); it consumes 130 mW when being driven [23]. The EDLC voltage when operating the device should be 2.5-2.8 V.

Assuming the energy consumption of the device is around 0.3 J, the required capacity is 380 mF. Therefore, this experiment used an EDLC of 440 mF. The leakage current, I_3 , of the EDLC was calculated to be $6.615 \cdot 10^{-7} \text{ A}$ from the voltage change over 24 hours with both ends of the capacitor open. The power consumption when the MPU is on is $60 \mu\text{W}$, so it is possible to ensure consistent operation using the power obtained from the received optical power (described later). However, in the prototype, the MPU is set to sleep mode and the device is powered off unless instructed by the CO in order

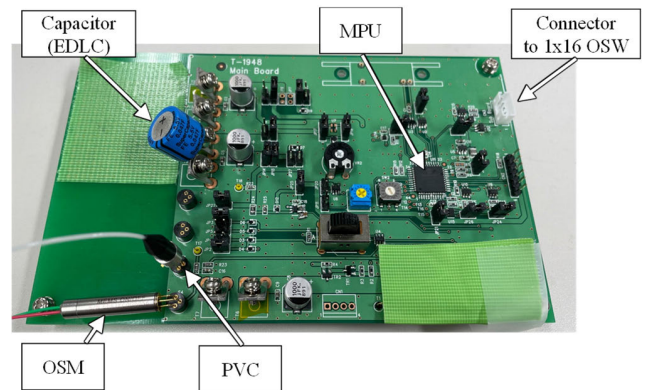


FIGURE 7. Prototype remote node.

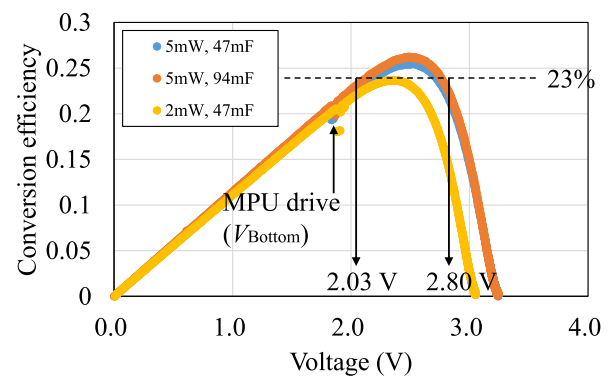


FIGURE 8. Photoelectric conversion efficiency versus the voltage of the PVC in the remote node.

to reduce the charge time and increase the discharge time as much as possible.

B. CONTROL PARAMETERS

LD operation is controlled by V_H and V_L . These parameters are determined to suit the conversion efficiency of the PVC in order to reduce the wastage of optical power. Fig. 8 shows measured and calculated results of the photoelectric conversion efficiency versus the applied voltage of the PVC employed in the prototype. The measurements were carried out by switching the light power received by PVC between 2 and 5 mW with EDLC capacity between 47 and 94 mF. It was confirmed that the photoelectric conversion efficiency of the PVC installed in the remote node prototype was not affected by the capacitance of the capacitor, but was affected by the received optical power. In order to keep the photoelectric conversion efficiency high, this study set the target efficiency at 23% when receiving 5 mW of optical power. As a result, V_H and V_L were determined to be 2.03 V and 2.80 V, respectively. Since V_{Bottom} of the MPU is 1.8 V, the power supply margin was 0.2 V.

C. COMPARING EXPERIMENTAL TO ESTIMATED RESULTS

The estimated results are compared to the experimental values in Fig. 9. The optical power received by the PVC

was 5 mW and EDLC capacity was 440 mF. In the experiment, the EDLC was charged by PoF from the state of zero charge, and the LD was stopped when the EDLC voltage reached 2.8 V. While the LD was stopped, the MPU was kept in sleep mode ready to receive instructions from CO. From the comparison, when the estimated value of the state of charge was 2.8 V, the experimental value was 2.65 V, so the error was 6%. After 16.7 hours V_L fell below the discharge state and reached 2.03 V, while the estimated value was 2.23 V, so an error of 10%. These errors suggest that the charge/discharge characteristics of the proposed circuit model and the fabricated remote node do not exactly match. In particular, the self-discharge characteristic of the EDLC appear to be the greatest concern, because the error seems to be large in the initial stage of discharge. It is known that the self-discharge characteristics of EDLCs vary widely depending on the charging method [24]. However, the slopes of the estimated and experimental curves are in good agreement in the latter region of discharge, and it is considered that the proposed PoF system is feasible with some corrections. It is possible to maintain the high photoelectric conversion efficiency of 23% or more by correcting the estimated voltage by communicating with the remote node a number of times. For example, when the estimated value reaches V_H while charging or when 8 hours have passed in the discharging state. In addition, according to this result, since the LD can be turned off for 16.4 hours while the total operating time of the PoF system is 16.6 hours, the LD can be turned off for more than 98.8% of the total operating time of the PoF system. A comparison of the ECE achieved by the PoF system with and without intermittent operation is shown in Table 1. The LD output power and capacitor capacitance are 5 mW and 440 mF, respectively. Energy levels without intermittent operation are derived by calculation. It takes 733 s more than the experimental value in Fig. 9 for the operation time of the LD to increase from the capacitor voltage of 2.03 V to 2.8 V. Therefore, the energy provided by the LD is 3.67 J. It was experimentally measured that 69.4 μ J was consumed by driving MPU and OSM in one communication cycle to obtain the capacitor voltage value. For example, when communication is performed once every 10 s, the energy charged to the capacitor by 5962 communication cycles decreases by 413.4 mJ from the stored energy for 1 charge/discharge cycle of 59626 s. On the other hand, in the PoF system with intermittent operation, if voltage correction is performed twice during charging and once during discharging, the error in the estimated voltage value of the capacitor can be suppressed to 5% or less. At this time, the charging time becomes 727.5 s, and the energy provided by the LD becomes 3.64 J. For 1 charge/discharge cycle, the energy consumption of the MPU is about 1 mJ including three communication cycles. Therefore, the energy that can be stored in the capacitor is as shown in Table 1, and the ECE of the PoF system with and without intermittent operation is 22.4% and 11.0%, respectively; the efficiency is more than doubled.

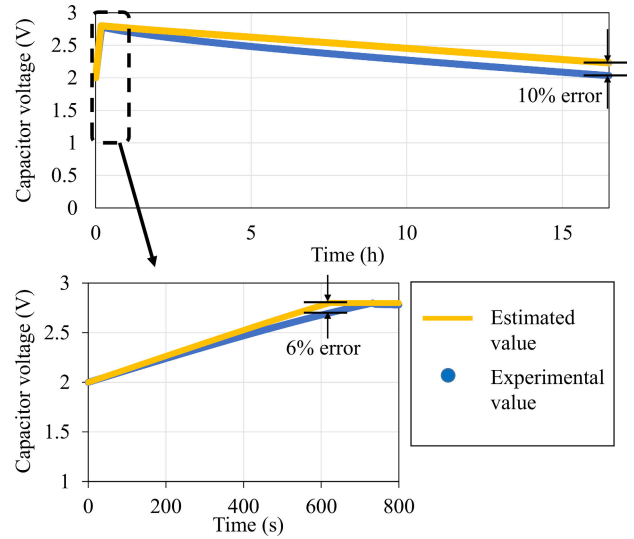


FIGURE 9. Comparing estimated and experimental results.

TABLE 1. Comparison of energy charging efficiency of PoF system with and without intermittent operation.

	Energy provided by LD (J)	Energy charged in Capacitor (J)	ECE (%)
PoF system without intermittent operation	3.67	0.405	11.0
Proposed PoF system with intermittent operation	3.64	0.817	22.4

If ECE is doubled, the target energy can be attained in half the time, which doubles the utilization cycle of the electric device.

IV. IMPLEMENTATION OF PROPOSED SYSTEM

We experimentally confirmed if an electrical device could be driven using the PoF system. Therefore, we constructed a system to drive a 1×16 optical switch (OSW) and checked its actual operation. The 1×16 OSW was implemented in the device section of the remote node as shown in Fig. 10. The CO side controller performed on-off LD control. Moreover, the light of the LD was modulated by the controller to generate the 1×16 OSW control signal that was transmitted at 110 bps. The LD light was transmitted over SMF and branched by a 90:10 optical coupler. The light receiving power of PVC was 5mW. After receiving the control signal on the MPU side, the DC/DC converter was driven by the MPU to boost the voltage of the capacitor to 5 V and supply operating voltage to the device. At this time, the LSW is turned on only while the 1×16 OSW is operating and receiving power. When operation was completed, the LSW was turned off and a signal indicating completion of the operation was sent to the CO side through the OSM. The capacitor used for

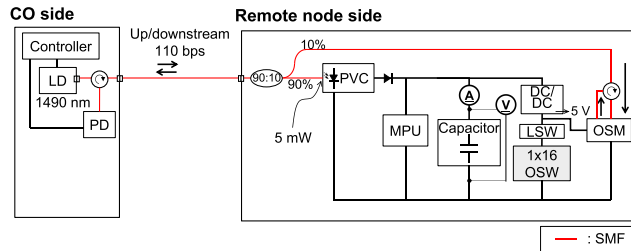


FIGURE 10. Experimental set-up.

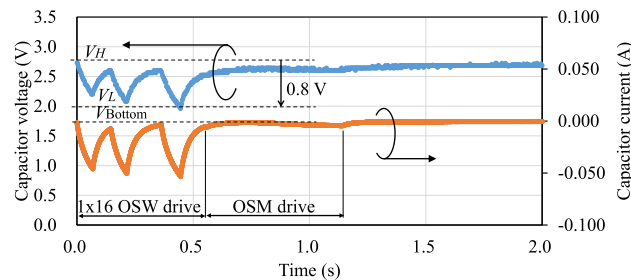


FIGURE 11. Capacitor voltage and current operating 1×16 optical switch. The capacitor current value is positive in the direction flowing into the capacitor and negative in the direction flowing out of the capacitor.

driving the 1×16 OSW was a 440 mF EDLC. The minimum driving voltage V_{Bottom} of the MPU is 1.8 V. Fig. 11 shows the capacitor voltage and current when the 1×16 OSW was operating. While charging, when 2.8 V was reached, a 1×16 OSW control signal was immediately transmitted from the CO side to activate the switch. When the operation was completed, a completion report was sent to the CO side through the OSM. The switch operation and completion report were completed in about 1 s in total. Furthermore, since the capacitor voltage after driving the 1×16 OSW must be larger than V_L and the capacitor voltage during driving 1×16 OSW must be larger than V_{Bottom} , the operation of the 1×16 OSW was carried out immediately upon reaching 2.8 V in this experiment. From the experimental results, 1×16 OSW operation time was 0.55 s, and the average power consumption of 1×16 OSW and MPU combined was 115 mW. The capacitor voltage after 1×16 OSW operation was 2.7 V, indicating that the photoelectric conversion efficiency is high, even after the device is driven. The total energy consumed, 0.121 J, includes OSM driving, and it takes 84 s (estimated) time to recharge from 2.7 V to 2.8 V at 5 mW receiving optical power of PVC. Considering that the operation time of the electrical device is 1 s and the assumed receiving optical power is more than 5 mW, it is found that the shortest cycle to operate the 1×16 OSW is less than 85 s. Additionally, an instantaneous voltage drop of 0.8 V was observed during the operation of the 1×16 OSW, as shown in Fig. 11. Despite this drop, the capacitor's voltage was maintained above 2.0 V, exceeding the V_{Bottom} of 1.8 V. This demonstrates that the 1×16 OSW can maintain stable operation without powering down the MPU.

V. CONCLUSION

We proposed a PoF system with intermittent operation control. It was found that the prototype could operate while maintaining the photoelectric conversion efficiency above 23%. By estimating the capacitor voltage and communicating the actual values occasionally, it was found that intermittent operation can be performed while reducing the power consumption of the remote node. The ECE per charge/discharge cycle is expected to be improved from 11.0% in our original PoF system to 22.4% in the proposed PoF system. Furthermore, it was found that high photoelectric conversion efficiency can be maintained even when driving the node's electrical device. As a result, it is possible to considerably reduce the need to poll the remote node for its capacitor voltage value, and so ensure that the LD was inactive for at least 98.8% of the operation time of the system. This suggests that the system can be operated continuously to support multiple remote nodes connected to one LD. This research establishes the intermittent operation control technology of PoF systems that offer energy savings and thus are environmentally friendly.

ACKNOWLEDGMENT

The support of Kazunori Katayama is acknowledged.

REFERENCES

- [1] J. D. López-Cardona, M. Delgado, R. Altuna, I. García, A. Núñez-Cascajero, M. Hinojosa, P. C. Lallana, I. Lombardero, A. Fresno, L. Cifuentes, and X. Barrero, "Optimized power-over-fiber system to remotely feed smart nodes for low-power consumption applications," in *Proc. 13th Spanish Conf. Electron Devices (CDE)*, 2021, pp. 41–44.
- [2] J. D. López-Cardona, C. Vázquez, D. S. Montero, and P. C. Lallana, "Remote optical powering using fiber optics in hazardous environments," *J. Lightw. Technol.*, vol. 36, no. 3, pp. 748–754, Feb. 1, 2018.
- [3] A. P. Goutzoulis, J. M. Zomp, and A. H. Johnson, "Development and antenna range demonstration of an eight-element optically powered directly modulated receive UHF fiberoptic manifold," *J. Lightw. Technol.*, vol. 14, no. 11, pp. 2499–2505, Nov. 1996.
- [4] D. Wake, A. Nkansah, N. J. Gomes, C. Lethien, C. Sion, and J.-P. Vilcot, "Optically powered remote units for radio-over-fiber systems," *J. Lightw. Technol.*, vol. 26, no. 15, pp. 2484–2491, Aug. 1, 2008.
- [5] C. Lethien, D. Wake, B. Verbeke, J.-P. Vilcot, C. Loyez, M. Zegaoui, N. Gomes, N. Rolland, and P.-A. Rolland, "Energy-autonomous picocell remote antenna unit for radio-over-fiber system using the multiservices concept," *IEEE Photon. Technol. Lett.*, vol. 24, no. 8, pp. 649–651, Apr. 15, 2012.
- [6] H. Kuboki and M. Matsuura, "Optically powered radio-over-fiber system based on center- and offset-launching techniques using a conventional multimode fiber," *Opt. Lett.*, vol. 43, no. 5, pp. 1067–1070, 2018.
- [7] M. Matsuura and Y. Minamoto, "Optically powered and controlled beam steering system for radio-over-fiber networks," *J. Lightw. Technol.*, vol. 35, no. 4, pp. 979–988, Feb. 15, 2017.
- [8] C. Vázquez, J. D. López-Cardona, P. C. Lallana, D. S. Montero, F. M. A. Al-Zubaidi, S. Pérez-Prieto, and I. Pérez Garcilópez, "Multicore fiber scenarios supporting power over fiber in radio over fiber systems," *IEEE Access*, vol. 7, pp. 158409–158418, 2019.
- [9] T. Umezawa, P. T. Dat, K. Kashima, A. Kanno, N. Yamamoto, and T. Kawanishi, "100-GHz radio and power over fiber transmission through multicore fiber using optical-to-radio converter," *J. Lightw. Technol.*, vol. 36, no. 2, pp. 617–623, Jan. 15, 2018.
- [10] C. Vázquez, D. S. Montero, F. M. A. Al-Zubaidi, and J. López-Cardona, "Experiments on shared- and dedicated-power over fiber scenarios in multi-core fibers," in *Proc. 28th Eur. Conf. Netw. Commun. (EuCNC)*, Valencia, Spain, 2019, pp. 412–415.

- [11] J. D. López-Cardona, R. Altuna, D. S. Montero, and C. Vázquez, "Power over fiber in C-RAN with low power sleep mode remote nodes using SMF," *J. Lightw. Technol.*, vol. 39, no. 15, pp. 4951–4957, Aug. 1, 2021.
- [12] M. Matsuura, H. Nomoto, H. Mamiya, T. Higuchi, D. Masson, and S. Fafard, "Over 40-W electric power and optical data transmission using an optical fiber," *IEEE Trans. Power Electron.*, vol. 36, no. 4, pp. 4532–4539, Apr. 2021.
- [13] O. López-Lapeña and J. Polo-Cantero, "Time-division multiplexing for power and data transmission on optical fibers," *IEEE Internet Things J.*, vol. 9, no. 18, pp. 17785–17792, Sep. 2022.
- [14] M. Roeger, B. Hiba, J. Hehmann, M. Straub, H. Schmuck, M. Hedrich, T. Pfeiffer, C. Koos, J. Leuthold, and W. Freude, "In-service monitoring of PON access networks with powerline independent devices," *J. Opt. Commun. Netw.*, vol. 6, no. 11, pp. 1018–1027, Nov. 2014.
- [15] *Safety of Laser Products—Part 2: Safety of Optical Fibre Communication Systems*, Standard IEC 60825-2, 2021.
- [16] C. Diouf, V. Quintard, L. Ghisa, M. Guegan, A. Pérennou, L. Gautier, M. Tardivel, S. Barbot, V. Dutreuil, and F. Colas, "Design, characterization, and test of a versatile single-mode power-over-fiber and communication system for seafloor observatories," *IEEE J. Ocean. Eng.*, vol. 45, no. 2, pp. 656–664, Apr. 2020.
- [17] Q. Mei, X. Gu, R. Shen, G. Li, Y. Li, and Y. Qin, "Meteorological monitoring system for transmission line tower based on power-over-fiber," in *Proc. 6th Int. Conf. Energy, Electr. Power Eng. (CEEPE)*, Guangzhou, China, May 2023, pp. 37–41.
- [18] T. Kawano, T. Manabe, A. Kuroda, K. Nakae, H. Watanabe, and K. Katayama, "Control using power-over-fiber for remote-operated optical fiber switching nodes," in *Proc. Int. Cable Connectivity Symp.*, 2022. [Online]. Available: https://iwcs.org/wp-content/uploads/2022/09/IWCS_2022_Final_Event_Program.pdf and <https://iwcs.conferencespot.org/event-data/pdf/catalystactivity34984/catalystactivitypaper20220826170406378bbe407b6bfb243a79876835b04d8f8be>
- [19] Y. Enomoto, H. Izumita, K. Mine, S. Urano, and N. Tomita, "Design and performance of novel optical fiber distribution and management system with testing functions in central office," *J. Lightw. Technol.*, vol. 29, no. 12, pp. 1818–1834, Jun. 15, 2011.
- [20] R. Komiya, K. Yoshida, and N. Tamaki, "The loop coverage comparison between TCM and echo canceller under various noise considerations," *IEEE Trans. Commun.*, vol. C-34, no. 11, pp. 1058–1067, Nov. 1986.
- [21] R. Kita, Y. Fukada, H. Katsurai, and T. Yoshida, "Accurately modeling optical power supply with low optical input power," *IEICE Commun. Exp.*, vol. 10, no. 12, pp. 979–984, Dec. 2021.
- [22] *DiCon Fiberoptics*. Accessed: Apr. 9, 2024. [Online]. Available: <https://www.diconfiberoptics.com/products/scd0046/SCD-0046G.pdf>
- [23] *Agiltron*. Accessed: Apr. 9, 2024. [Online]. Available: <https://agiltron.com/category/optical-switches/lightbend-fiber-optical-switches/>
- [24] S. Dinglasan-Fenol, F. S. Caluyo, and W. Sugimoto, "Effect of charging methods on self-discharge and leakage current of supercapacitors," in *Proc. 4th Int. Conf. Control Eng. Inf. Technol. (CEIT)*, Hammamet, Tunisia, Dec. 2016, pp. 1–5.



TOMOHIRO KAWANO received the B.E. and M.E. degrees in electrical and electronic engineering from Kyushu University, Fukuoka, Japan, in 2008 and 2010, respectively. In 2010, he joined the NTT Access Network Service Systems Laboratories, Nippon Telegraph and Telephone Corporation, Ibaraki, Japan, where he has been engaged in research on power-over-fiber techniques for optical access networks. He is a member of the Institute of Electronics, Information and Communication Engineers (IEICE), Japan.



RYO KOYAMA received the B.S. and M.S. degrees in precision engineering from The University of Tokyo, Tokyo, Japan, in 2001 and 2003, respectively. In 2003, he joined the Access Network Service Systems Laboratories, Nippon Telegraph and Telephone Corporation, Ibaraki, Japan, where he has been engaged in research on optical fiber wiring and splicing techniques for optical access networks. He is an Assistant Secretary of the IEC SC86B and a member of the Institute of Electronics, Information and Communication Engineers (IEICE), Japan.



AKIHIRO KURODA received the B.E. and M.E. degrees in science and engineering from Yamagata University, Yonezawa, Japan, in 2013 and 2015, respectively. In 2015, he joined East Nippon Telegraph and Telephone Corporation. In 2021, he joined the NTT Access Network Service Systems Laboratories, Nippon Telegraph and Telephone Corporation, Ibaraki, Japan. Recently, he has been engaged in the research and development of power-over-fiber systems.



TAKUI UEMATSU received the B.E. and M.E. degrees in electronic engineering from Hokkaido University, Sapporo, Japan, in 2012 and 2014, respectively. In 2014, he joined the Access Network Service Systems Laboratories, NTT Corporation, Ibaraki, Japan, where he has been engaged in research on optical fiber couplers and an optical fiber coupling technique. He is an Associate Distinguished Researcher of NTT and a member of the Institute of Electronics, Information and Communication Engineers (IEICE), Japan. He is also a member of TC86/SC86B preparing international standards for fiber-optic interconnecting devices and passive components at the International Electrotechnical Commission (IEC).



CHISATO FUKAI received the B.E. and M.E. degrees in functional materials science and the Ph.D. degree from Saitama University, Saitama, Japan, in 1999, 2001, and 2014, respectively. In 2001, she joined Access Network Service Systems Laboratories, NTT Corporation, Ibaraki, Japan, where she has engaged in research on optical fiber and its splicing techniques. She is a member of the Institute of Electronics, Information and Communication Engineers (IEICE), Japan.



HIROSHI WATANABE received the B.E. and M.E. degrees in applied physics from The University of Tokyo, Japan, in 1996 and 1998, respectively, and the Ph.D. degree in engineering from Hokkaido University, in 2017. In 1998, he joined the NTT Access Network Service Systems Laboratories, Ibaraki, Japan, where he engaged in optical measurement and maintenance technologies for optical fiber networks. His current research interest includes power-over-fiber systems. He is a member of the Institute of Electronics, Information and Communication Engineers (IEICE), Japan.



IKUTARO OGUSHI received the B.E. and M.E. degrees in electrical engineering from Osaka University, in 2000 and 2002, respectively. In 2002, he joined NTT Access Network Systems Laboratories, Tsukuba, Ibaraki, Japan, where he engaged in research and development of an optical fiber line testing system for submarine cables and an optical fiber distribution system for use in central offices. He is currently a Senior Research Engineer and a Supervisor of the NTT Access Network Service Systems Laboratories. He is a member of the Institute of Electronics, Information and Communication Engineers, Japan.

...